Electronic Supporting Information
For

Effect of Flexible Linker Length in 3,4-Ethylenedioxythiophene Derivatives for Solid State Polymerization

Tusy chuong, Kai Peng, Lili Huang, Jiangbin Xia*

College of Chemistry and Molecular Science, Wuhan University, Wuhan 430072, China

Corresponding author. E-mail: jbxia@whu.edu.cn

Tel & Fax: 86-27-67856707

Contents

1. ^{1}H-NMR and ^{13}C-NMR spectra of the compounds

Figure S1. ^{1}H NMR ($CDCl_3$) spectrum of **Bis-(7-iodo-2,3-dihydro-thieno[3,4-b][1,4]dioxin-5-ylmethyl)-methyl-amine (Br_2-3-EDOT, 1)**

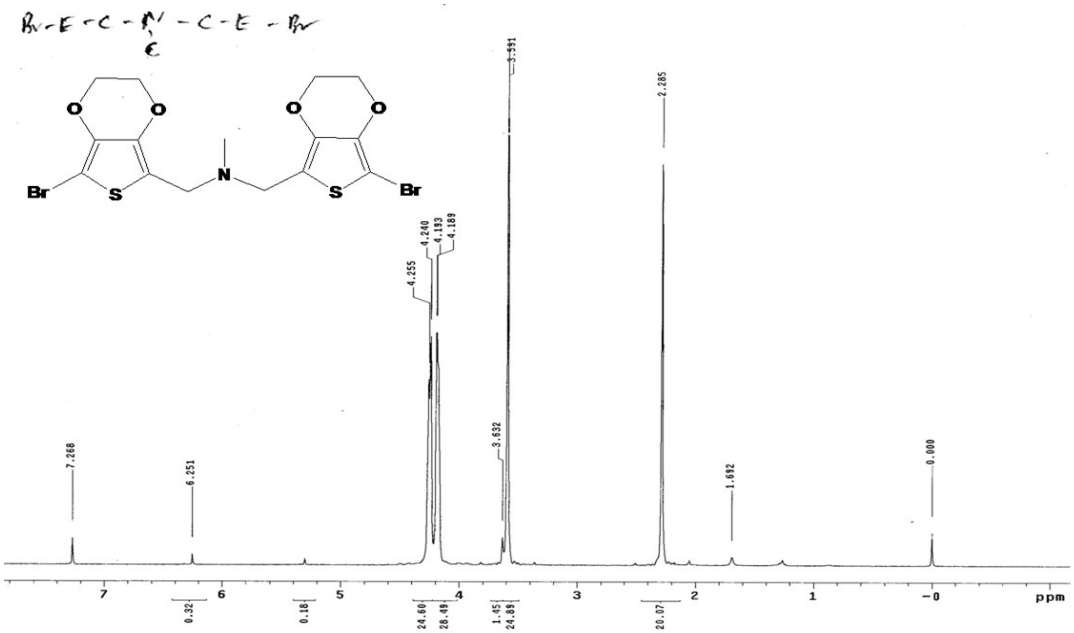

Figure S2. ^{13}C NMR ($CDCl_3$) spectrum of **Bis-(7-iodo-2,3-dihydro-thieno[3,4-b][1,4]dioxin-5-ylmethyl)-methyl-amine (Br_2-3-EDOT, 1)**

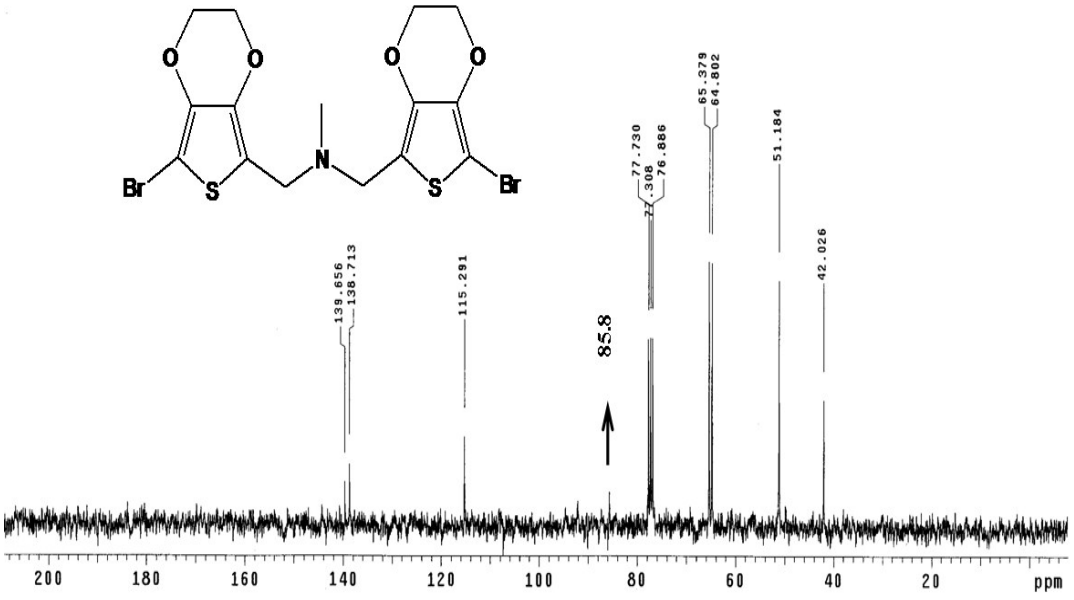

Figure S3. ^{1}H NMR ($CDCl_3$) spectrum of **Bis-(7-iodo-2,3-dihydro-thieno[3,4-b][1,4]dioxin-5-ylmethyl)-methyl-amine (I_2-3-EDOT, 2)**

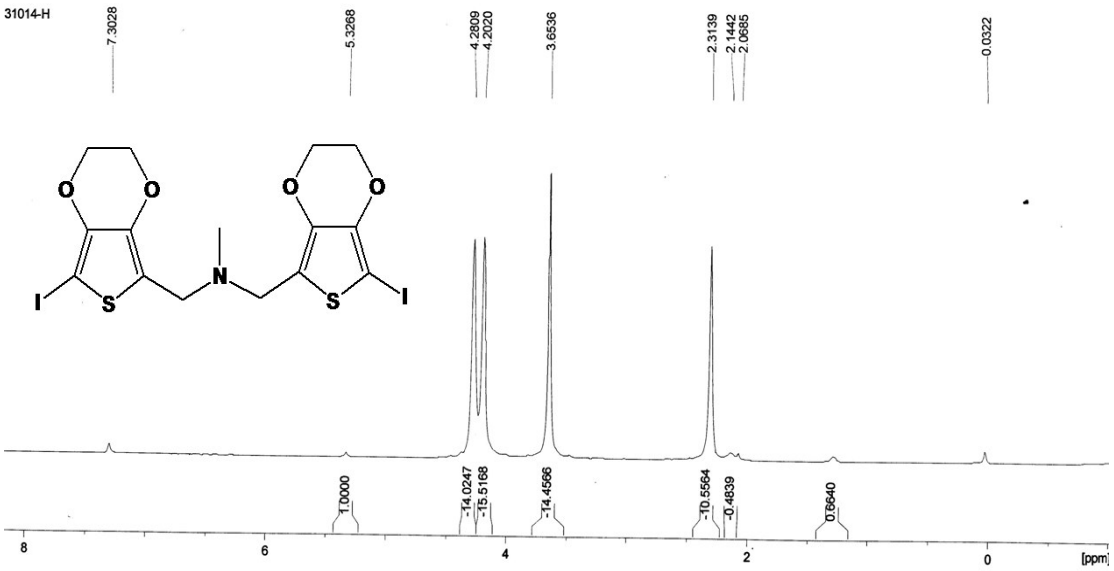

Figure S4. ^{13}C NMR ($CDCl_3$) spectrum of **Bis-(7-iodo-2,3-dihydro-thieno[3,4-b][1,4]dioxin-5-ylmethyl)-methyl-amine (I_2-3-EDOT, 2)**

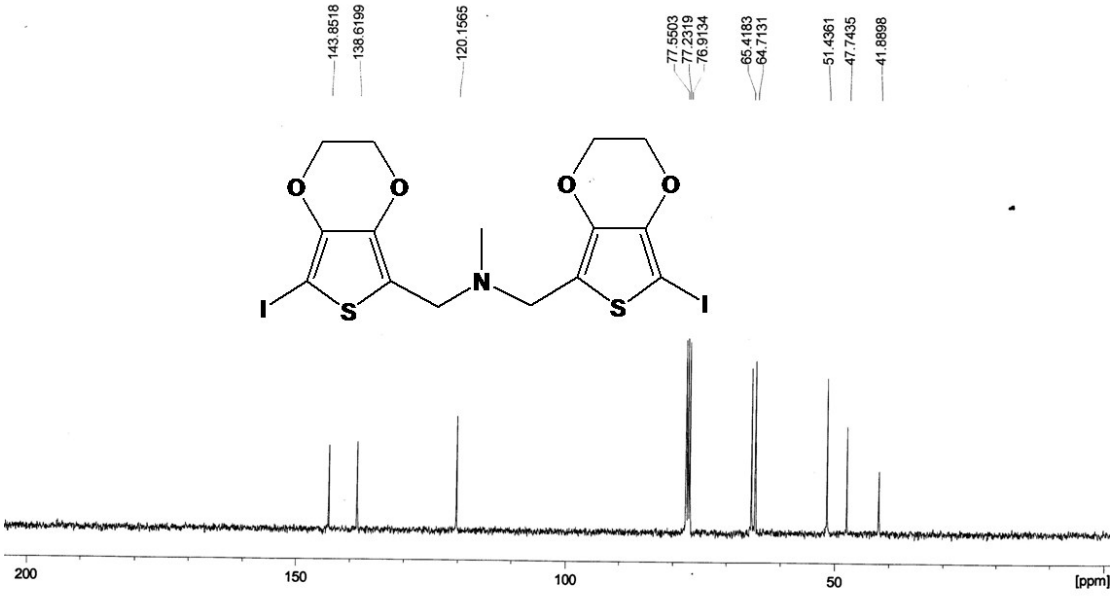

Figure S5. ^{1}H NMR ($CDCl_3$) spectrum of **Butyl-bis-(7-iodo-2,3-dihydro-thieno[3,4-b][1,4]dioxin-5-ylmethyl)-amine (I_2-3-butyl-EDOT, 3)**

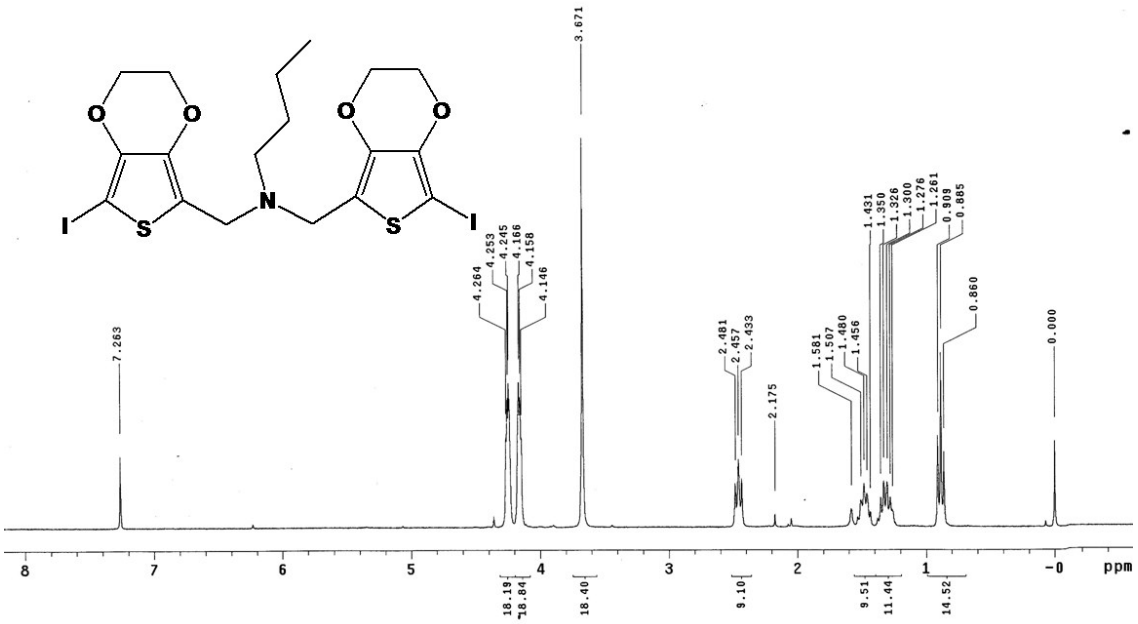

Figure S6. ^{13}C NMR ($CDCl_3$) **Butyl-bis-(7-iodo-2,3-dihydro-thieno[3,4-b][1,4]dioxin-5-ylmethyl)-amine (I_2-3-butyl-EDOT, 3)**

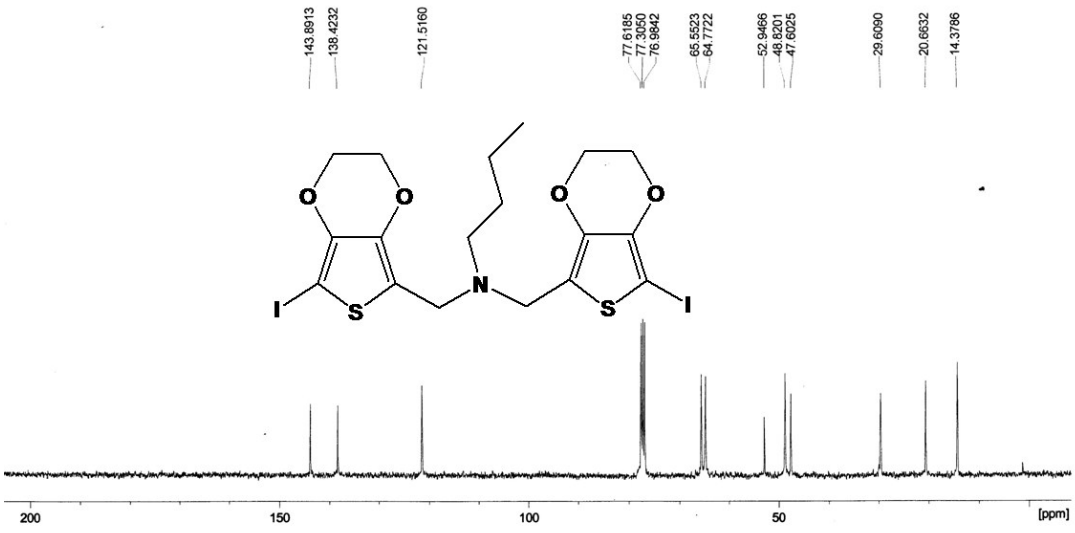

Figure S7. ^{1}H NMR ($CDCl_3$) spectrum of **1,2-Bis-(7-iodo-2,3-dihydro-thieno[3,4-b][1,4]dioxin-5-yl)-bis-dimethylsilanyl-methane (I_2-4-EDOT, 4)**

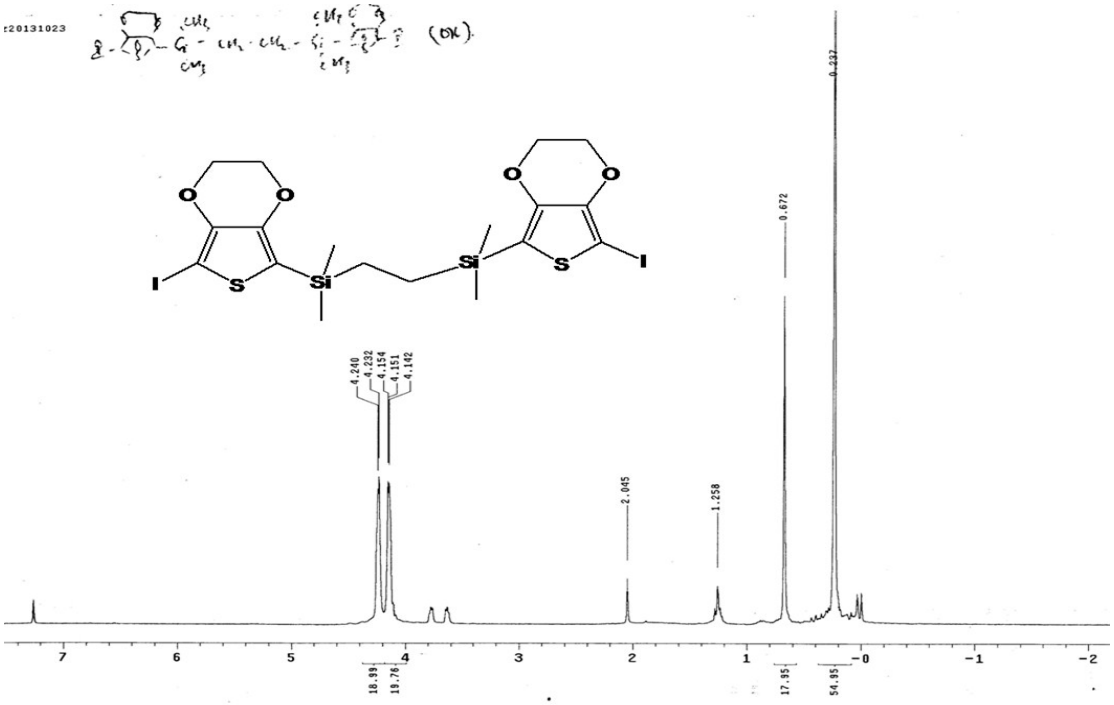

Figure S8. ^{13}C NMR ($CDCl_3$) **1,2-Bis-(7-iodo-2,3-dihydro-thieno[3,4-b][1,4]dioxin-5-yl)-bis-dimethylsilanyl-methane (I_2-4-EDOT, 4)**

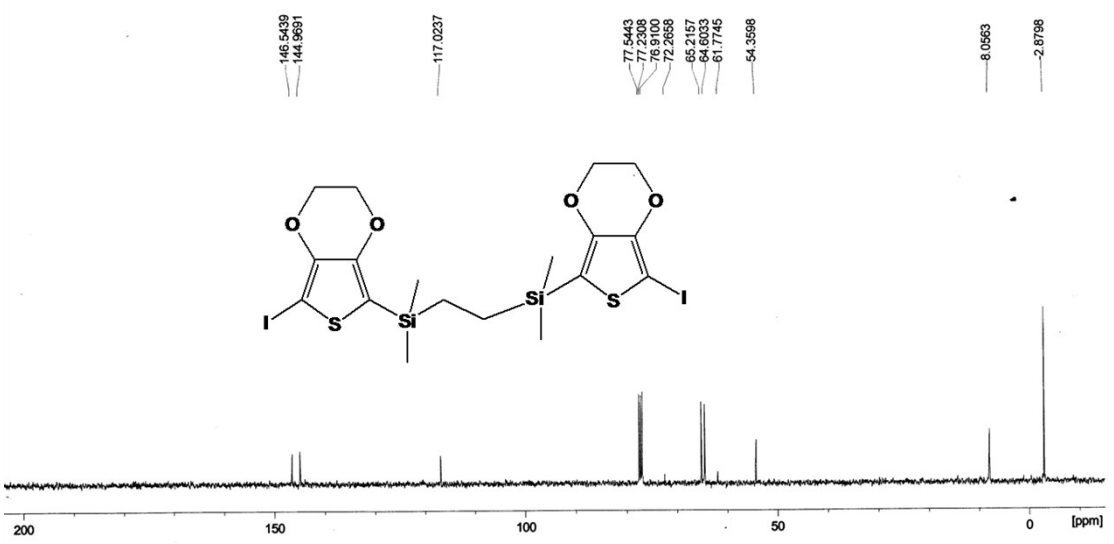

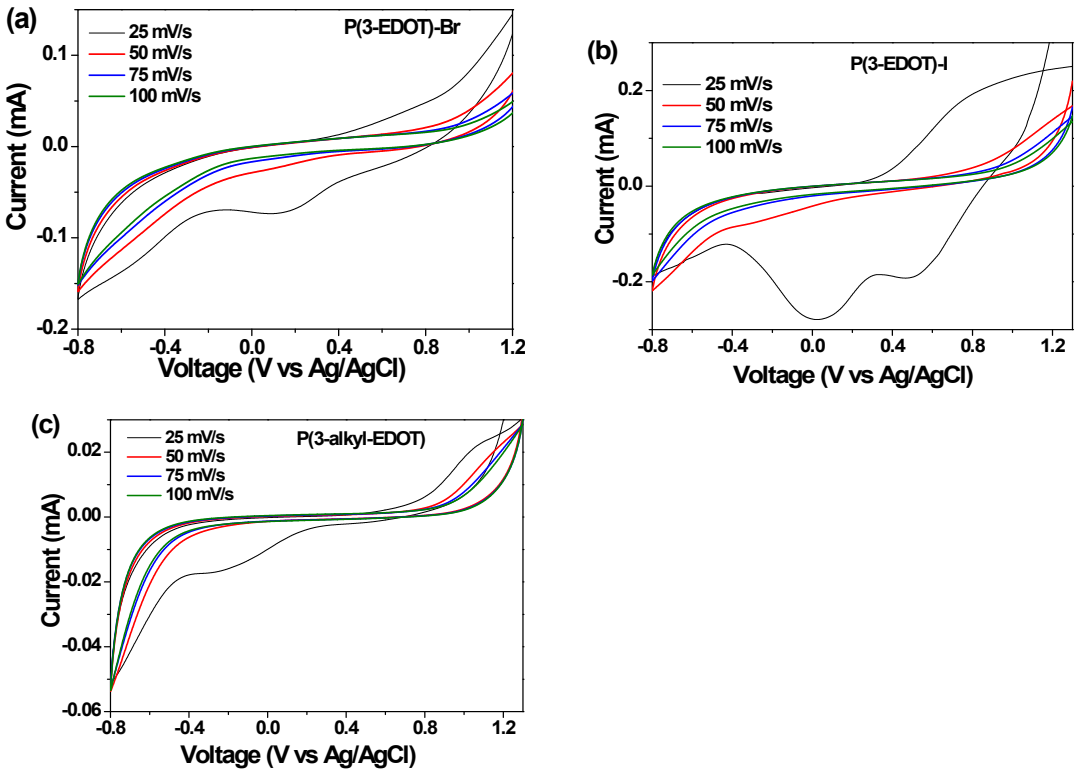

2. Figure S9. The CVs of the polymers film in acetonitrile solution containing 0.1 M Bu_4NClO_4 taken at various scan rates.

Cyclic Voltammetry behavior of the polymers

As we can see that all three polymers' CV curves show similar shapes and are quite different with that of traditional PEDOT's and those of having one flexible atom of C or Si.[7] The latter systems usually show wide and reverse redox behavior of the thiophen chain around region of -0.5-0.6 V. In addition, their first scan at scan rate of 25 mV/s shows typical redox behavior while most peaks disappear in the following scans. We attribute such phenomena to the nonreversible redox behavior due to non-conjugation of thiophene unit, revealing that all of them are not good candidates for charge storage. Once they are stable enough, their onset oxidation potential are nearly same with 0.8 V vs/Ag/AgCl, which are assigned to N oxidation[1,2] in the polymer matrix. Meanwhile, the abrupt reduction near -0.2 to -0.8 V region are assigned to the nitrogen's reduction process. Therefore, we attributes their higher oxidation potentials to the non-conjugation in the polymer chain with downshift of HOMO level, which resulted in poor electrochemical properties. Generally, it is easy to extract HOMO/LUMO information and bandgap from CV due to the involving similar electron obtain and lost. As we discuss in the above section, these polymers Abs spectra reveal that all of them show non-oxidation state under iodine, which are consisted with their CV behavior.

1. T. L. Macdonald, W. G. Gutheim, R. B. Martin, F. P. Guengerich. *Biochem*. **1989**, *28*, 2071.
2. J. W. Arbogast, C. S. Foote, M. Kao, *J. Am. Chem. Soc.* **1992**, *114*, 2277.

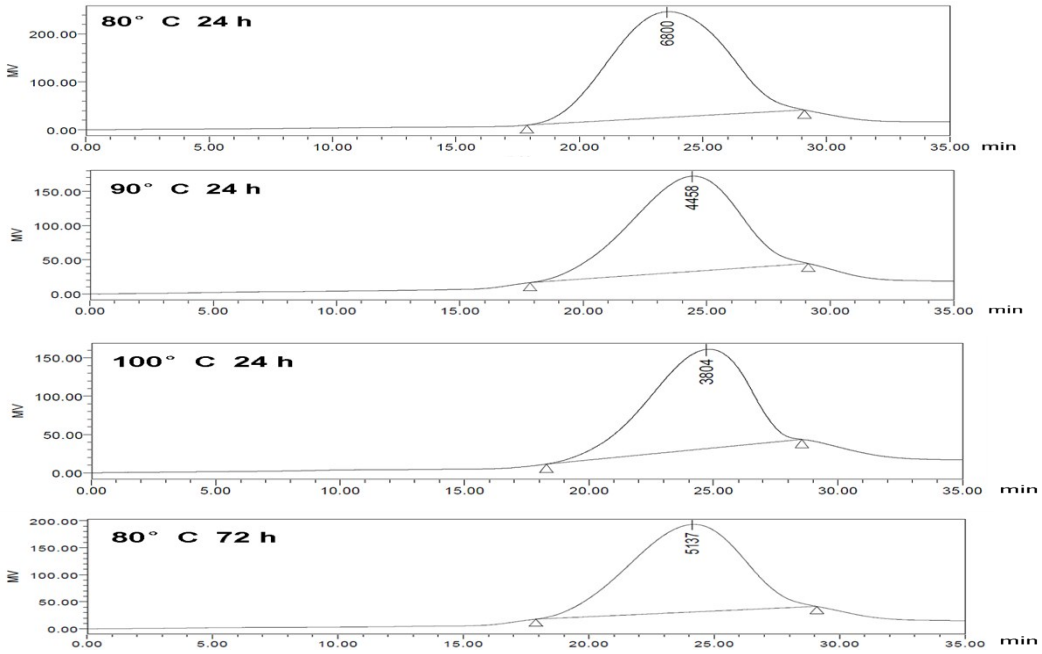

3 Figure S10. GPC profiles of P(3-alkyl-EDOT) obtained under different temperatures.

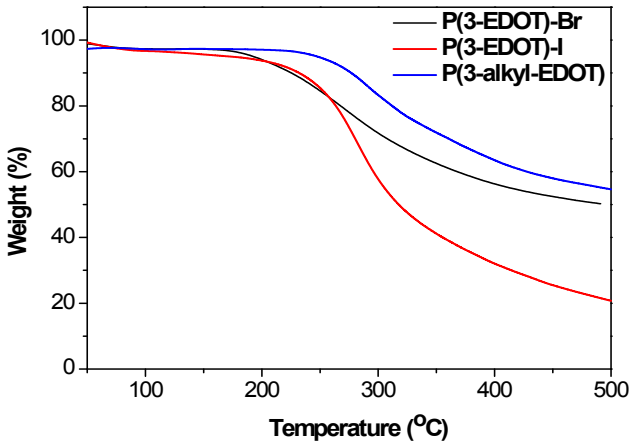

4. Figure S11. TGA curves of the polymers with a heating rate of 10°C min^{-1} under nitrogen.

The 5% weight-loss temperatures for P(3-EDOT)-Br, P(3-EDOT)-I and P(3-alkyl-EDOT) were 193**,** 185 and 248°C respectively, indicating that the introduction of alkyl chain would enhance thermal stability greatly. In addition, it seems that P(3-EDOT)-I shows less stability compared with P(3-EDOT)-Br. We attribute this to its lower repeat units with high halogen content in the chain, resulting further halogen release under thermal treatment.

5. Table S1. Details of the Data Collection and Structure Refinements for All Monomers Reported in This Work

parameter	Br_2-3-EDOT	I_2-3-EDOT	I_2-3-alkyl-EDOT	I_2-4-EDOT
empirical formula	$C_{15}H_{15}Br_2N_4S_2$	$C_{15}H_{15}I_2NO_4S_2$	$C_{18}H_{21}I_2NO_4S_2$	$C_{18}H_{24}I_2O_4S_2Si_2$
fw	497.22	591.20	633.28	678.49
cryst syst	triclinic	Triclinic	Tetragonal	monoclinic
space group	P-1	P-1	P-42(1)c	P21/c
a (Å)	7.7337(5)	7.8257(11)	23.3143(14)	17.5004(7)
b (Å)	10.1482(7)	10.5383(14)	23.3143(14)	7.2281(3)
c (Å)	11.8659(8)	11.8883(16)	8.1165(5)	19.8464(8)
α (deg)	84.846(2)	83.995(2)	90	90
β (deg)	71.451(2)	71.977(2)	90	96.182(1)
γ (deg)	77.611(2)	78.365(2)	90	90
V ($Å^3$)	862.10(10)	912.2(2)	4411.8(5)	2495.86(18)
Z	2	2	8	4
D_{calcd} (g/cm^3)	1.912	2.152	1.907	1.806
cryst size (mm^3)	0.17×0.09×0.27	0.30×0.29×0.24	0.12×0.10×0.10	0.10×0.16×0.20
diffractometer	Bruker APEX-II CCD	SMART CCD	Bruker APEX-II CCD	Bruker APEX-II CCD
F(000)	492	564	2448	1320
T (K)	173(2)	293(2)	296(2)	173(2)
θmax	28.36	28.44	30.55	28.23
reflns collected	7646	5996	6749	6120
indep reflns	4150	3759	5949	5236
param refined	236	219	264	253
R_1, wR_2	0.0432, 0.1217	0.0356, 0.0891	0.0269, 0.0644	0.0248, 0.0577
GOF (F2)	1.010	1.047	1.027	1.048